International Journal of Multiphysics
Volume 18, No. 1, 2024
ISSN: 1750-9548

An Experimental Study Comparing the Effects of Adipose Derived Stem Cells and Platelet Rich Plasma on Wound Healing in Rats

Ahmed Magdy Mahmoud[1], Amr Magdy Sayed Mahmoud[1], Fatma Abd ElKarim Al Zaki Abu-Zahra[2], Zainab Mohammad Altaib Ahmad[3,] Dina Farouk El Sayed Elnaggar[4]

1 Plastic, Burn and Maxillofacial Surgery Department, Faculty of Medicine, Ain Shams University, Egypt

2 Biochemistry Department, Faculty of Medicine, Ain Shams University, Egypt

3 Histology Department, Faculty of Medicine, Helwan University, Egypt

4 Plastic, Burn and Maxillofacial Surgery Department, Faculty of Medicine, Helwan University, Egypt

***Corresponding author:** Ahmed Magdy Mahmoud

Email: ahmaj64@gmail.com,

Abstract:

Background: Large or chronic wounds may hinder the complex biological process of wound healing because of insufficient cellular resources and a poor regeneration response. Because of their ability to promote angiogenesis, collagen deposition, and tissue repair, platelet-rich plasma (PRP) and adipose-derived stem cells (ADSCs) have drawn more attention as regenerative treatment options. This experimental study aimed to compare the effects of ADSCs and PRP on wound healing in rats.

Methods: This experimental study was conducted on forty male albino rats. Ten rats were used as donors for ADSCs and PRP preparation, while thirty rats were divided into three study groups: Group I included 12 rats treated with ADSCs, Group II included 12 rats treated with PRP, and Group III included 6 control rats. Standardized wounds were created and evaluated at predetermined time points. Wound healing was assessed on days 3, 5, 7, and 14 using computerized image analysis software to measure wound surface area and calculate the wound-healing rate. Statistical comparison between groups was performed using mixed-design ANOVA.

Results: The survival of rats was uneventful apart from four mortalities during wound follow-up, which were replaced. A statistically significant difference in wound healing was found between all groups at all assessed time points ($p<0.001$). The ADSCs-treated group showed the highest mean healing percentage throughout the study, followed by the PRP-treated group, while the control group showed the lowest healing rate. On day 14, the mean healing rate reached 94.08% in the ADSCs group, 86.42% in the PRP group, and 71% in the control group. Healing significantly increased over time within each group ($p<0.001$).

Conclusion: Both ADSCs and PRP significantly enhanced wound healing in rats compared with the control group. ADSCs demonstrated superior wound-healing effects compared with PRP at all studied time points, suggesting that ADSCs may represent a more effective regenerative option for accelerating wound repair.

Keywords: Adipose-derived stem cells; Platelet-rich plasma; Wound healing; Rats; Regenerative medicine; Experimental study.

Introduction:

Skin that is intact serves as a barrier of defense against the outside world. An organized series of biochemical processes is initiated to heal the injured skin when the barrier is breached (1). However, because there are insufficient cell sources, big skin wounds and chronic wounds cannot adequately heal themselves (2).

Because mesenchymal stem cells (MSCs) are multipotent stromal cells that may differentiate into a range of cell types, such as osteoblasts, chondrocytes, myocytes, adipocytes, and skin cells (3), they may be the best alternative cell source for the healing of skin wounds. Adipose-derived stem cells (ADSCs) are the most often utilized of the many MSC kinds (4).

One great source of MSCs is adipose tissue. The cellular yield of ADSCs is 100–1000 times higher than that of bone mesenchymal stem cells (BMSCs), and their isolation is incredibly easy and effective (5).

It has been demonstrated that ADSCs can participate in and support the regeneration process either directly or indirectly (via their paracrine function, which releases growth factors and cytokines) (6). Additionally, by promoting collagen deposition and angiogenesis, they can be employed to improve wound healing (7).

A concentrate of platelet-rich plasma protein made from whole blood that has been centrifuged to exclude red blood cells is known as platelet-rich plasma (PRP). Platelet-derived growth factor (PDGF), transforming growth factor beta (TGF-β), fibroblast growth factor (FGF), insulin-like growth factor 1 (IGF-1), insulin-like growth factor 2 (IGF-2), vascular endothelial growth factor (VEGF), epidermal growth factor (EGF), interleukin 8 (IL-8), keratinocyte growth factor (KGF), and connective tissue growth factor (CTGF) (8).

Therefore, PRP has been used in a number of professions, including plastic surgery, dentistry, orthopaedics, and dermatology, to promote a quick healing response (2).

Materials and Methods

This study was done between April 2021 and September 2023. It was conducted at The Medical Ain Shams Research Institute Animal Facility (MASRI – animal facility) associated with Ain Shams' Faculty of Medicine and approved from the Research Ethics Committee (REC) of Faculty of Medicine, Ain Shams University.

Materials

A. Reagents:

1. Dulbecco's modified Eagles medium (DMEM) with high glucose (4,5g/L), L-glutamine, and no sodium pyruvate (Lonza; Catalog #12-604F [500ml], Swiss).
2. FBS (Seralab®, UK).
3. Collagenase NB4 standard grade, 0.2% (SERVA Electrophoresis, Catalog # 17454, Germany).
4. Antibiotics and anti-mycotics: Penicillin G (10,000 units/mL), streptomycin sulfate (10,000 µg/mL), and Amphotericin B (25 mcg/mL) in 0.85% NaCL solution (Lonza, catalog # 17-745H, Swiss).
5. Phosphate buffered saline (PBS) without calcium and magnesium at pH 7.4 (Lonza; catalog # 17-516F, Swiss).
6. Trypsin/EDTA (Lonza, catalog #CC-3232, Switzerland).
7. Trypan blue 0.4% solution (Lonza, catalog #17-942E, Swiss).

B. Equipment:

1. **Biosafety Cabinet (BSC), Class II, Type A2** (NUAIRE; NU-425-600, USA) (fig 1)

Figure 1: The Biosafety Cabinet; BSC.

2. **Centrifuge;** (Hettich universal 16, USA) (fig 2).

a b

Figure 2: a) the centrifuge device b) the screen of the centrifuge showing RPM and time.

3. **CO2 Incubator**; (NUAIRE; Autoflow NU-4750 Water Jacket Laboratory CO2 Incubator, USA) (fig 3)

Figure 3: Water Jacket Laboratory CO2 Incubator

4. **Inverted Microscope**; (Zeiss Axiovert 100 Phase Contrast Microscope, Germany) (Fig 4).

Figure 4: The inverted microscope

5. **Shaking 37 ◦c Water bath** (Uamatn BT25)

6. **Light Microscope**

C. Supplies:

1. Electric pipet filler/dispenser (5 and 10 mL).
2. Hemocytometer with cover slip.
3. Sterile pipets (5 and 10mL).
4. Tissue culture flasks 25 cm2 (Easy Flask, Nunc, Roskilde, Denmark).
5. Sterile Petri dish 3 and 10 ml.
6. Falcon tubes 15 ml (Nalge Nunc, Roskilde, Denmark)

D. Working Solution:

The medical research center team recreated Complete Culture Medium (CCM) by adding 500 mL DMEM, 65 mL FBS (final conc. 13%), and 1.5% antibiotic and anti-mycotic mixture (Penicillin G (10,000 units/mL), Streptomycin sulfate (10,000 µg/mL), and Amphotericin B (25 mcg/mL) in a solution of 0.85% NaCL (instead of 10% FBS & 1% antibiotic/antimycotic as described by Lu et al. (9). After passing through a sterile 0.22 µm filter, CCM is separated into aliquots and kept at 4 °C. The aliquots were warmed to 37 °C before to the experiment.

E. Surgical Instruments:

Dissector, disposable waterproof drapes, toothed forceps, scalpel No. 15 with handle, and needle holder.

F. Animal model:

The following standards should be met by the best animal model for producing critical size defects (CSDs) for bone work: ***(10).***

1. Inexpensive.

2. Easy to handle.

3. Adequate bone volume:

Adequacy indicates that the deficiency will not mend on its own and that the remaining skeleton is stable, preventing fracture, particularly if the defect is full thickness and contains both cortical and cancellous bone.

4. Comparable histological and physiological characteristics, such as membranous bone to the bone under study.

5. It is simple to perform histopathological and radiographic tests on the animal.

Rat models are helpful in studies pertaining to bones. Rats are also better than rabbits. Ileus and post-antibiotic diarrhea are less likely to occur (11).

Therefore, albino rats were the best suitable for this study. In addition to meeting the aforementioned requirements, the calvarium is a non-stress location with a lower risk of infection.

There were 42 male albino rats employed, which is the bare minimum needed to finish this investigation. Rats were acquired from the animal lab connected to the Medical Research Center at Ain Shams University's Faculty of Medicine after being approved by the CARE (Committee on Animal Research and Ethics) and given two weeks to acclimate. They were kept in cages of four rats each, with free access to food and water, enough ventilation, and a climate that was regulated to 22°C with 12-hour intermittent light/dark cycles. The most skilled investigator handled the rats. There was no hardship, worry, or agony involved. Anesthesia was used for all procedures and the collection of bodily material. The rats were put to death by anesthetic overdose at the conclusion of the experiment, and the remains of their bodies were burned. The rats are divided into two models: -

Model 1: (Donor rats for adipose derived stem cells)

Ten rats of young (5-6weeks) male albino rats were used.

Model 2:

Thirty-two adult (6-7months) male albino rats weighing 260-340 grams were divided into four groups as follow: -

- **Group I (n=8):** with surgically created calvarial bone defect will be left without repair
- **Group II (n=8):** with surgically created calvarial bone defect will be repaired by allogenic DBM without cell seeding
- **Group III (n=8):** with surgically created calvarial bone defect will be repaired by allogenic DBM seeded by ASCs
- **Group IV (n=8):** with surgically created calvarial bone defects will be repaired by prolene mesh seeded by ASCs

Methods

The following steps were the main steps in the study:

- **Step 1**: preparation of Scaffolds (DBM and prolene mesh)
- **Step 2**: Harvesting inguinal pad of fat.
- **Step 3**: Tissue processing.
- **Step 4**: Isolation, Culture and expansion of ADSCs.
- **Step 5**: Scaffold Seeding.
- **Step 6**: In vivo implantation.

- **Step 7**: Harvest of specimen.

Step 1: Preparation of Scaffolds (DBM and prolene mesh)

I) Preparation of prolene mesh:

Using an 8 mm biopsy punch, a 30x30 cm prolene mesh was divided into tiny, symmetrical, circular segments (scaffolds) with an 8 mm diameter (Figure 5). Every section was sterilized and stored independently.

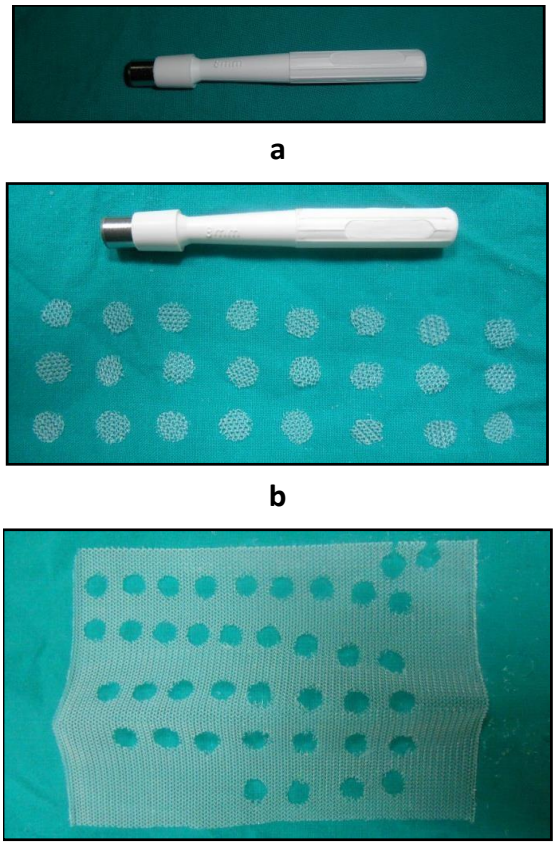

Figure 5: The preparation of prolene mesh; a) 8mm biopsy punch. b) Prolene mesh was cut by punch into multiple small pieces (scaffolds). c) prolene mesh with multiple holes after obtaining multiple rounded scaffolds sized 8 mm all around.

II) Preparation of DBM:

Group II (reconstructed by DBM without cell seeding) and Group III (reconstructed by DBM with cell seeding) received demineralized bone from Group I (control) and Group IV (reconstructed by prolene mesh and ADSCs), respectively.

Rats were given intramuscular injections of ketamine (1-2 mg/kg) to induce anesthesia, which was maintained as needed. The rat was covered with a disposable waterproof drape after the surgical incision site (the right parietal area) was cleaned with povidone iodine and 70% alcohol under sterile conditions using a razor and lubricant. The right parietal bone was exposed by making a 2 cm incision along the sagittal suture and dissecting the skin, muscles, and periosteum. The 8mm biopsy punch was then carefully used to create a circular defect that measured 8 mm all around in order to prevent damage to the dura mater (Fig 6).

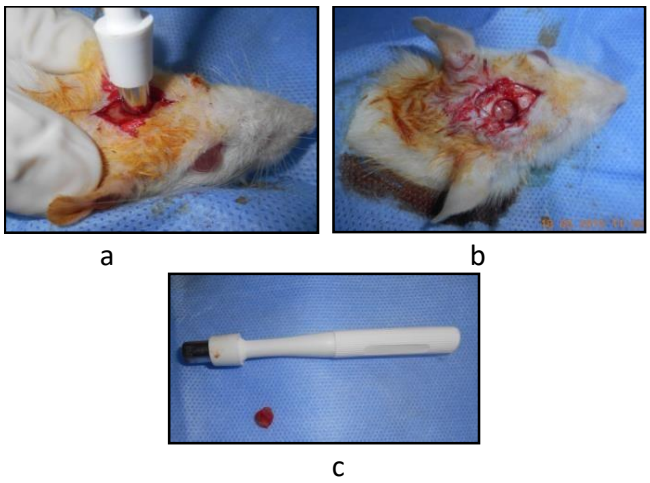

Figure 6: Harvest of an 8mm circular bone from rats calvaria; a) circular bone excised by 8mm biopsy punch. b) dura intact after bone harvest. c) harvested bone is circular measuring 8mm all around.

Process of demineralization:

The extracted bone segments (Fig. 7) were promptly placed in a 0.6 N HCL solution and kept at 4°C for 72 hours. Every 24 hours, the HCL was replaced. The bone segments were then cleaned with distilled water for eight hours while being constantly stirred to eliminate the acid.

While still submerged in alcohol, each section will be kept independently in tiny plastic tubes at minus 70°C (Fig 8).

Figure 7: The harvested Bony segments are collected in a petri dish and are ready for demineralization.

Figure 8: The Demineralized bone scaffolds are immersed in alcohol.

Step 2: Harvesting inguinal pad of fat.

Ten young male albino rats (56 weeks) were employed as donors for adipose-derived stem cells (Animal model 1). This was the bare minimum of animals. An intramuscular dose of ketamine (1-2 mg/kg) will be used to anesthetize each donor rat, and they will be kept as needed.

Strict sterility was adhered to. The rat was covered with disposable waterproof drapes after the surgical wound site was cleaned with povidone iodine and 70% alcohol after being shaved with a razor and lubrication. The surgical area (inguinal regions) of the rat was oriented toward the surgeon (Fig 9).

Figure 9: Positioning of the rat with the surgical area facing the surgeon; the dashed lines represent the incision line at both inguinal regions.

Incisions were made in both inguinal folds (Fig. 10). After meticulous dissection and isolation, the inguinal fat was quickly moved to a sterile petri dish (Fig. 11). A 4.0 absorbable suture (vicryl) is used to seal the wounds.

Figure 10: Both inguinal folds are incised and dissected with isolation of the inguinal pad of fat.

Figure 11: The harvested inguinal pad of fat collected in a petri dish.

Step 3: Tissue processing.

Strict aseptic conditions were maintained during the culture process, with all supplies and reagents being sterile, all materials utilized inside the laminar flow Biosafety cabinet (BSC) being cleaned with 70% alcohol, and the culture media being preheated to 37°C. Every employee was donning lab coats and gloves.

In a laminar flow BSC, the extracted fat was cleaned by phosphate buffered saline (PBS) and sliced into pieces with a diameter of about 1-2 mm (Figs. 12 & 13). After that, the tissue will be rinsed three times for five minutes in PBS.

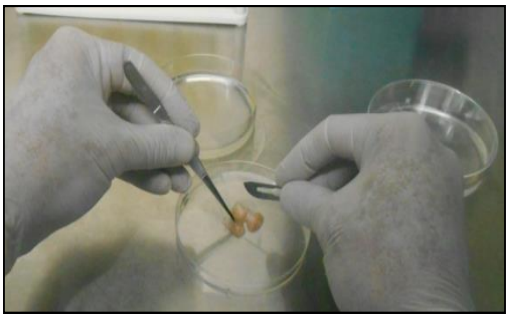

Figure 12: The harvested fat was cut into pieces of approximately 1-2 mm diameter inside a laminar flow biosafety cabinet.

Figure 13: Petri dishes containing the minced fat

Step 4: Isolation, Culture and expansion of ADSCs.

1. Isolation:

In order to begin the digestion process, the chopped fat was combined with 0.2% collagenase type I in a 25 ml falcon tube and vigorously shaken for 40 minutes at 37°C in a water bath shaker. The fat turned into a uniform mixture (Fig. 14).

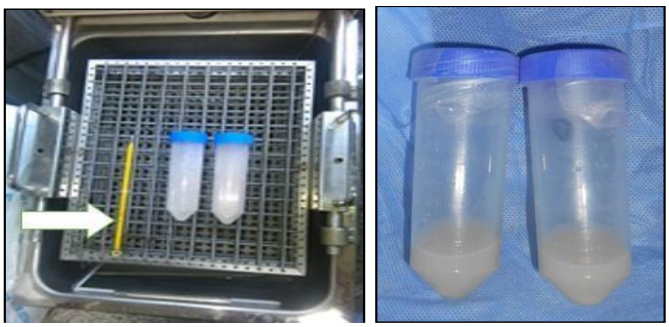

a b

Figure 14: Falcon tubes containing the mixture of minced fat and collagenase type I in a water bath shaker at 37°C; a) the arrow pointing to the thermometer b) the homogenous fat solution at the end of shaking process.

The collagenase was neutralized by adding an equal volume of CCM. The cell suspension was then centrifuged for five minutes at 1300 rpm. Following centrifugation, the supernatant that contained connective tissue and mature adipocytes was properly disposed of using a pipet. Stromal vascular fraction (SVF) is the term for the cell pellet that forms at the bottom (Fig. 15). To lyse the red blood cells, the cell pellet was resuspended in 10 milliliters of CCM.

Figure 15: The cell suspension after centrifugation with the cell pellet (SVF) at the bottom (marked by an oval).

2. Culture:

The cell pellet will be cultivated at 37°C, 5% CO2, and 100% RH in a 25 cm2 culture flask with CCM in a CO2 incubator (Fig. 16). Every seventy-two hours, the medium was changed. After discarding the non-adherent cells, PBS was used to wash the adherent cells.

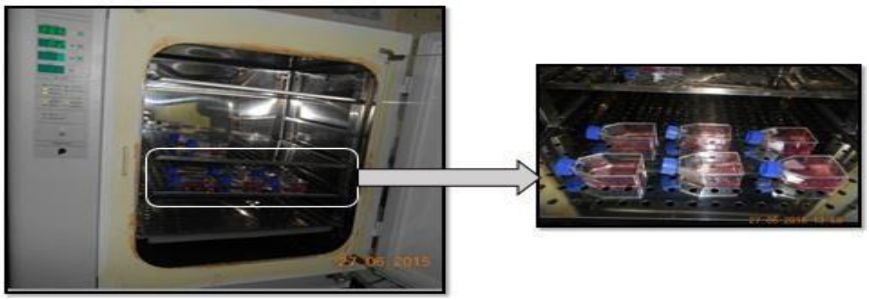

Figure 16: The culture flasks inside the CO2 incubator.

3. Expansion:

The inverted microscope was used to monitor the cell expansion (Figs. 17, 18, and 19). On the twelfth day after passage zero, the cells were taken at 80–90% confluence, or cell density. Using a micro-scrubber and 0.25% trypsin-EDTA, the cultivated cells were separated from the culture flasks (Fig. 20). After five minutes, the cell separation was confirmed by further observation under an inverted microscope.

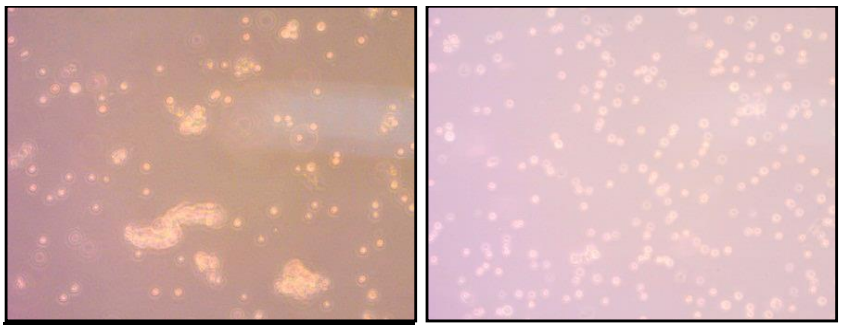

a b

Figure 17: Passage zero; the cells appearance under the inverted microscope (**X 100**). a) cell aggregate in clumps b) cells appeared as small rounded cells.

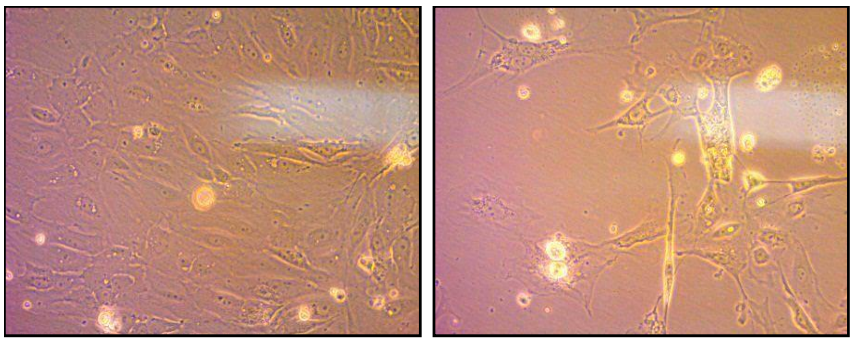

a b

Figure 18: Day 3; a) the cells appeared as spindle shaped cells b) under higher magnification (**X 200**).

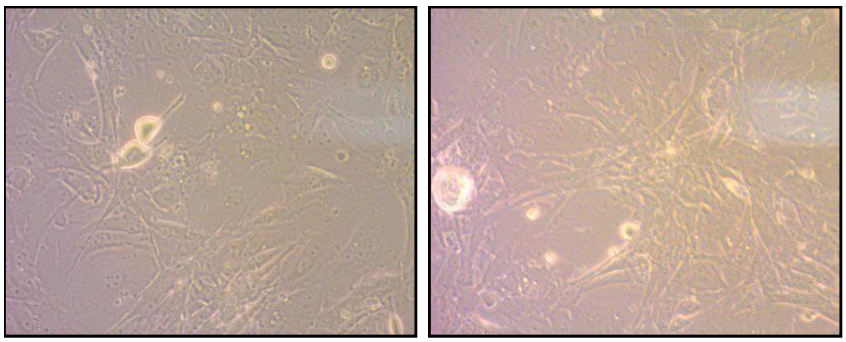

a **b**

Figure 19: Day 5; a) the cells are more confluent b) under higher magnification (**X 200**).

Figure 20: The microscrubber was used to detach the adherent cells to the culture flask at day 12.

- After adding an equivalent volume of CCM to counteract the effects of trypsinogen-EDTA, the cells were collected by centrifuging at 2000 rpm for five minutes at room temperature. The cells were then suspended in 1 milliliter of PBS.
- For five to fifteen minutes, 50 microliters of cell suspension were added to an equivalent volume of 0.4% trypan blue to confirm the cells' viability and counting. Only non-viable cells could be stained.
- A hemocytometer was used to calculate the viable cells in small 4 squares. The average for each square was then computed by dividing the sum by 4 and multiplying the result by 104. The number of viable cells per milliliter and the viability percentage are calculated using the following formula (the dilution factor used was 2).
- Viable cell count x dilution factor x 104 = number of viable cells/ml.

- Total viable cells (unstained) divided by total cells x 100 is the viability percentage.

Step 5: Scaffolds seeding.

The scaffolds wet by DMEM solution were seeded by a $3x10^6$ cells (Fig 21).

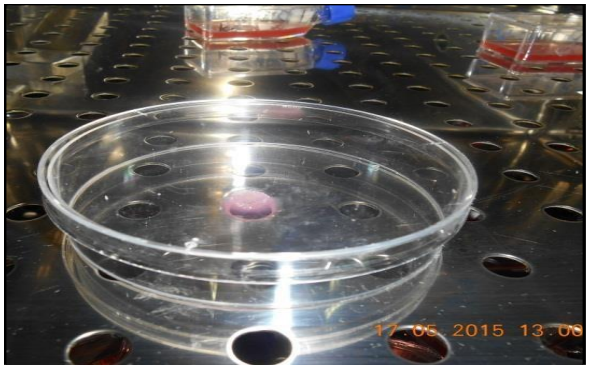

Figure 21: The scaffold was seeded with ADSCs.

Step 6: In vivo implantation.

Rats were given intramuscular injections of ketamine (1-2 mg/kg) to induce anesthesia, which was maintained as needed. The rat was covered with a disposable waterproof drape after the surgical incision site (the right parietal area) was cleaned with povidone iodine and 70% alcohol under sterile conditions using a razor and lubricant. The right parietal bone was exposed by making a 2 cm incision along the sagittal suture and dissecting the skin, muscles, and periosteum. The 8mm biopsy punch was then carefully used to create a circular defect that measured 8 mm all around in order to prevent damage to the dura mater. The rats were then split up into three groups:

Group II (n=8): with surgically created calvarial bone defect was repaired by allogenic DBM without cell seeding. The dimensions of the defect and the DBM are equal so, press fit is enough for fixation (Fig 22).

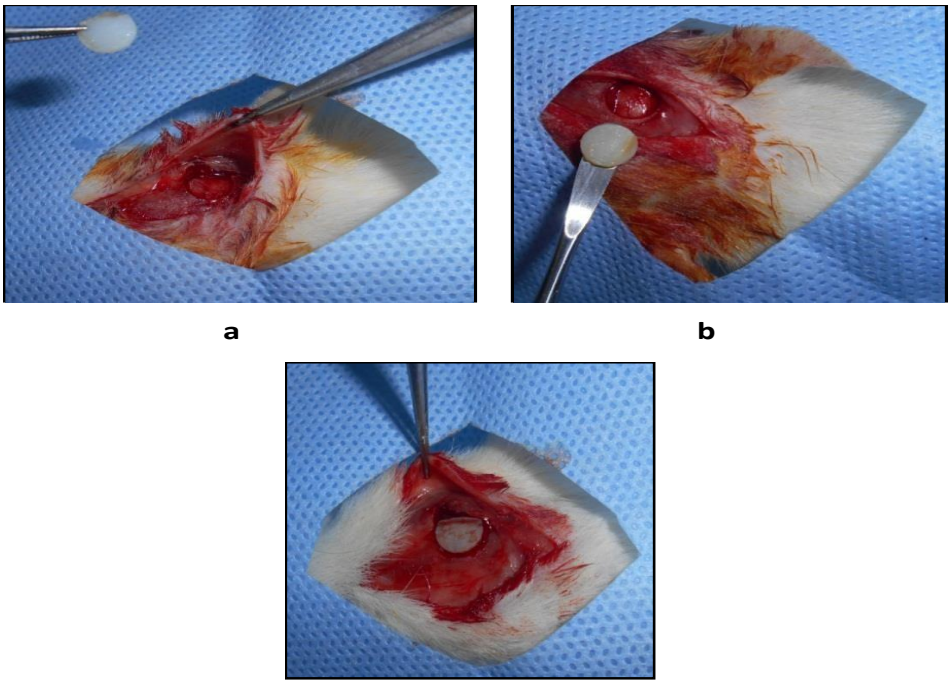

Figure 1: Group II with surgically created calvarial bone defect repaired by allogenic DBM without cell seeding; a) the skin, musculature and periosteum were dissected b) DBM ready for implantation c) DBM after implantation.

Group III (n=8): with surgically created calvarial bone defect was repaired by allogenic DBM seeded by ASCs. Also, There the no need for hardware for fixation as press fitting only is enough (Fig 23).

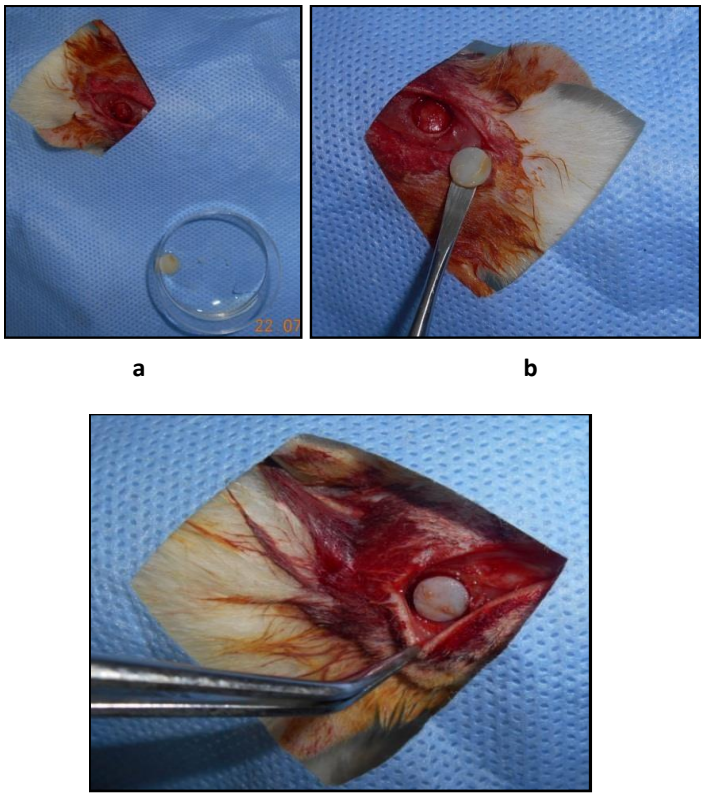

Figure 23: Group III with surgically created calvarial bone defect that was repaired by allogenic DBM seeded with ASCs; a) the defect created and the DBM seeded with ADSCs in a petri dish b) DBM seeded with ADSCs ready for implantation c) DBM seeded with ADSCs after implantation.

Group IV (n=8): with surgically created calvarial bone defects will be repaired by prolene mesh seeded by ASCs (Fig 24).

The periosteum, muscles and skin will be sutured back in all groups at the end of surgery.

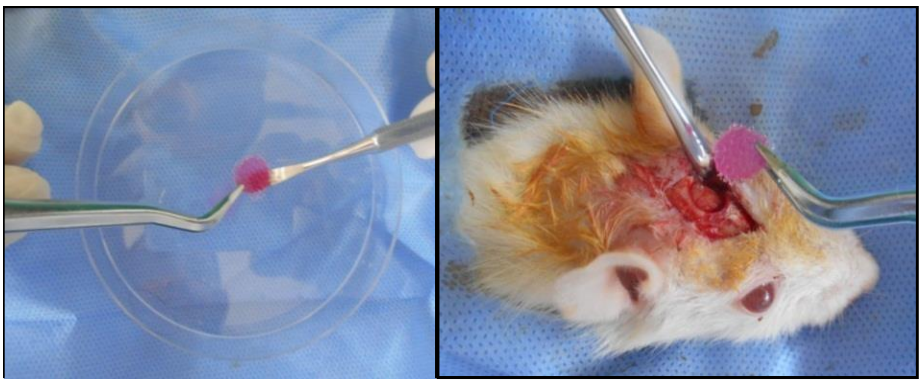

c d

Figure 24: Group IV with surgically created calvarial bone defect repaired with prolene mesh seeded by ASCs; a) prolene mesh seeded by ASCs in a petri dish b) prolene mesh seeded by ASCs ready for implantation c) prolene mesh seeded by ASCs implanted in the calvarial bone defect d) after wound closure.

Postoperative care:

1. **Rats Identification:**

Cage cards with the sex, age, date of intervention, investigator name, and contact number were used to identify the rats. Rat numbers were identified by ear punch labeling (Fig. 25).

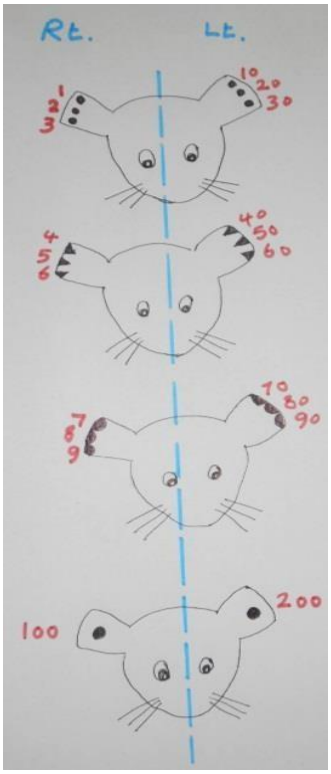

Group	Rat Number	
	from	To
Group I (control)	1	8
Group II (DBM)	9	16
Group III (DBM + ADSCs)	17	24
Group IV (Mesh + ADSCs)	25	32

Figure 25: Ear punch for rats labelling; complete circular punch at Rt. Ear marks for 1,2 and 3 for upper, middle and lower ear and at Lt. ear donates 10,20 and 30 respectively. Upper, middle and lower Rt. Ear Triangular punch marks for 4,5 and 6 but for Lt. ear means 40,50 and 60 respectively. Upper, middle and lower Rt. Ear semi-circular punch marks for 4,5 and 6 and for Lt. ear 70,80 and 90 respectively. Central complete circle at Rt. Ear marks for 100 and at Lt. ear 200.

2. **Analgesia:**

Rats were given 1 mg/kg/day of diclofenac sodium (NSAID) in water, and they were monitored for pain indicators such as anorexia (absence of fecal pellets), decreased appetite (few pellets), rubbing wounds, and restlessness.

3. **Antibiotics:**

Amoxicillin 10 mg/kg was administered with water twice daily for 21 days.

4. **Wound care:**

The surgical site was evaluated for inflammation, necrosis, hemorrhage or exudates.

Step 7: Harvest of the specimens.

Eight weeks following in vivo implantation, euthanasia was carried out by overdosing on anesthetic. Blocks containing the rebuilt defect and a rim of the surrounding calvarium were removed during the biopsies. (Fig 26).

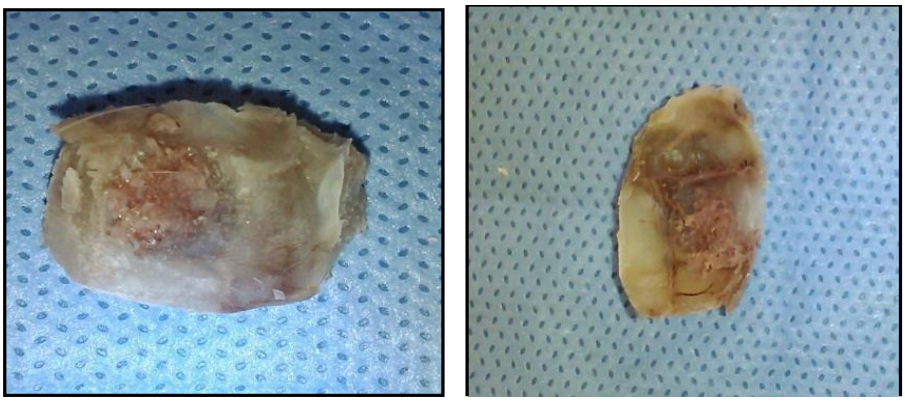

Figure 26: The specimen; blocks containing the defcet and a rim of the surrounding calvarium; a) outer aspect b) Inner aspect.

Results

In this study, Forty- Male albino rats were used. Ten of them were donor for ADSCs & PRP, and 30 were divided into 3 studying groups**.** The rat's survival at all studied groups was uneventful apart from Four mortalities during wound follow up (1 in **group I**, 1 in **group II** and 2 in **group III**). These rats were replaced (Fig 27).

The studied groups were:

- **Group-I:** ADSCs (N=12).
- **Group-II:** PRP (N=12).
- **Group-III:** Control (N=6).

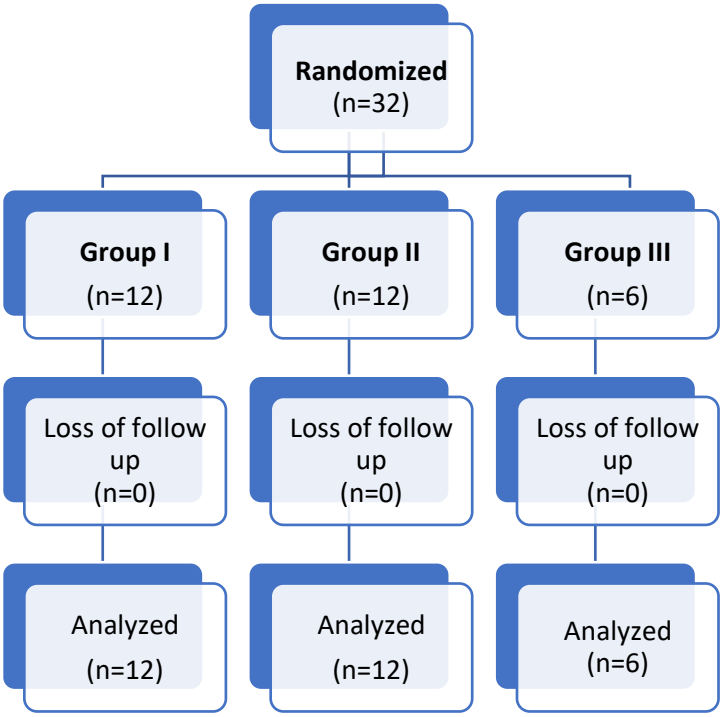

Figure 27: Study flow chart

1. Gross Evaluation at autopsy

The 3 studied groups are evaluated throughout a course of 2 weeks postoperatively before euthanasia (Fig 28). The defects were examined for the rate of wound healing through the equation: wound-healing rate = (the area of the original wound - the area of the unhealed wound)/the area of the original wound × 100%.

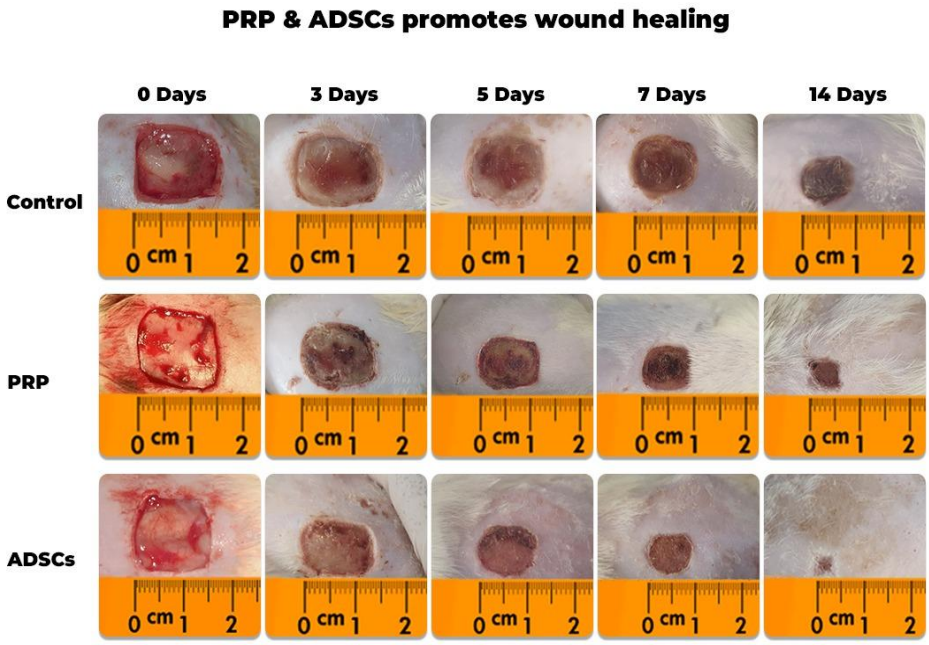

Figure 28: Gross evaluation of the studied groups at autopsy a) Group I b) Group II c) Group III; all at days 0,3,5,7,14 consecutively.

Image J

A version of software used for image analysis. In our study it helped to measure the surface area of wounds in the targeted stages in a computerized way, which in turn helped to compute the rate of wound healing in rats as the pattern of healing in of the wound edges in rats changes the square shaped wound into a more circular pattern.

The example in the following figures shows an example to measure the wound surface of a rat at day 7.

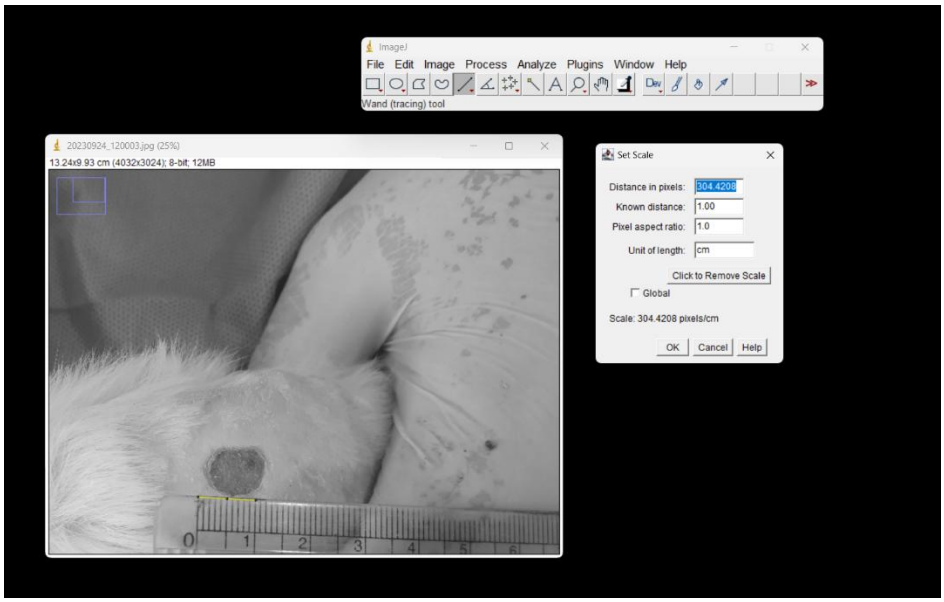

Figure 29: Shows first the process to set scale; A line (yellow) was drawn on the used ruler in the photo from zero to one cm to pick a real precise dimension; then the real length of the drawn line (1cm) was specified manually to allow the used software to standardize the real length unit used with a corresponding length in pixels; Thus the software was then be able to convert the virtual measurements (in pixels) to a corresponding real measurements (in centimeters).

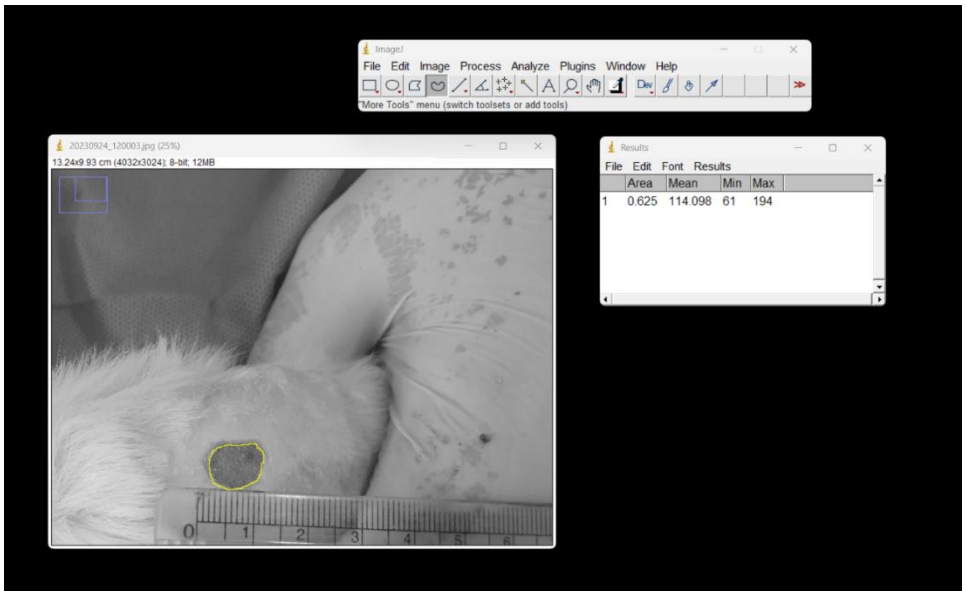

Figure 30: The wound area to be measured was marked manually then measured by the software in a computerized manner using the previous data input.

In the example, given the starting wound surface area (at day 0) was 2.25 cm2 (1.5cm×1.5cm), the rate of wound healing for this wound being measured at day 7 will be (2.25-0.625)/2.25×100 ≈ 72%.

Comparison between study groups regarding rate of healing:

Table 1: Rate of healing at the predetermined points of time in different groups.

Group I (ADSCs)

Rat Number	Day 3 (%)	Day 5 (%)	Day 7 (%)	Day 14 (%)
1	23	42	69	92
2	27	46	74	97
3	26	47	74	94
4	25	46	73	96
5	25	47	74	94
6	27	47	75	96
7	26	45	74	91
8	25	46	76	94
9	23	44	75	93
10	23	45	73	94
11	27	52	72	98
12	24	46	68	90

Group II (PRP)

Rat Number	Day 3 (%)	Day 5 (%)	Day 7 (%)	Day 14 (%)
1	20	41	58	85
2	23	42	65	90
3	21	39	58	86
4	20	38	67	84
5	18	39	58	89
6	19	38	69	90
7	18	48	68	88
8	20	40	55	83
9	19	38	60	89
10	21	41	72	91
11	21	38	59	86

12	20	38	55	76

Group III (Control)

Rat Number	**Day 3 (%)**	**Day 5 (%)**	**Day 7 (%)**	**Day 14 (%)**
1	12	30	48	70
2	14	33	42	82
3	9	34	49	73
4	14	32	42	68
5	14	28	42	76
6	10	29	53	57

Statistical methods:

Table 2: Mixed design ANOVA for the effect of time on healing among 3 different study groups

Healing		**Control**	**Group I**	**Group II**	**p value**	**sig.**
Day 3	Mean ± SE	12.17 ± 0.67	25.08 ± 0.48	20 ± 0.48	<0.001*	S
	95% CI	10.78 - 13.55	24.1 - 26.06	19.02 - 20.98		
Day 5	Mean ± SE	31 ± 1.06	46.08 ± 0.75	40 ± 0.75	<0.001*	S
	95% CI	28.83 - 33.17	44.55 - 47.62	38.47 - 41.53		
Day 7	Mean ± SE	46 ± 1.85	73.08 ± 1.31	62 ± 1.31	<0.001*	S
	95% CI	42.2 - 49.8	70.4 - 75.77	59.31 - 64.69		
Day 14	Mean ± SE	71 ± 1.94	94.08 ± 1.37	86.42 ± 1.37	<0.001*	S
	95% CI	67.02 - 74.98	91.27 - 96.9	83.6 - 89.23		
p value		<0.001**	<0.001**	<0.001**		
sig.		S	S	S		

Post hoc test:

*significant difference between all groups

**significant difference between all time points

The table displays the results of a mixed design ANOVA that looked at the percentage of healing in three separate groups (control, group I, and group II) at four time points (days 0, 5, 7, and 14). The main effects of group and time, as well as the interaction effect, were all significant ($p < 0.001$). The control group had the lowest percentage of healing at each time point, whereas Group I had the highest. Group II fell between the control and group I. All groups' healing percentages grew over time, however group I and group II increased at a higher rate than the control group.

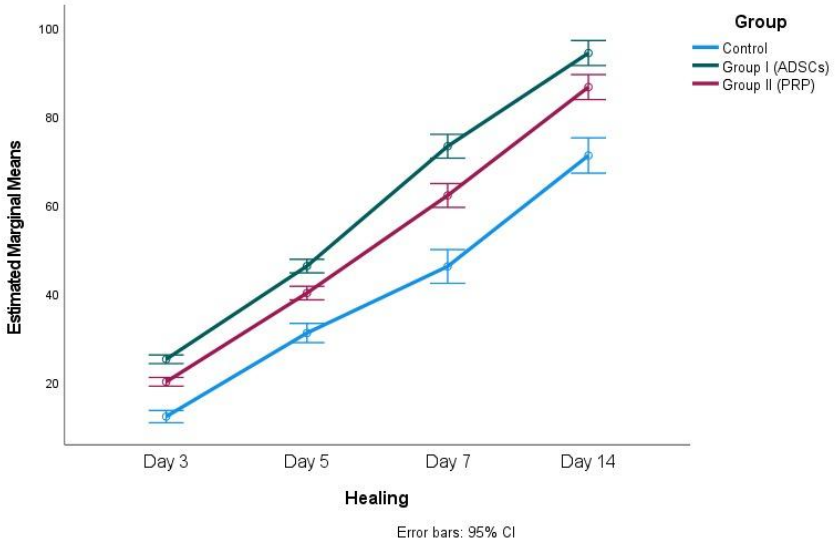

Discussion

The body is shielded from the outside world by intact skin. When the barrier is breached, a deliberate sequence of biological responses is set off to repair the damaged skin (12). However, severe skin wounds and chronic wounds cannot heal well on their own because there are insufficient cell sources available (13).

High protease activity in problematic wounds creates a pro-inflammatory milieu that reduces growth factors and chemokines needed for wound healing as well as the migration and proliferation of fibroblasts, which are essential for the development of new tissue (14).

Mesenchymal stem cells (MSCs) are multipotent stromal cells that can differentiate into a variety of cell types, including skin cells, osteoblasts, chondrocytes, myocytes, and adipocytes (15). As a result, they might be the best substitute cell source for repairing skin wounds. Adipose-derived stem cells (ADSCs) are the most widely utilized MSC type in dermatology (2).

One great source of MSCs is fat tissue (16). Compared to bone mesenchymal stem cells (BMSCs), ADSCs have a cellular yield that is 100–1000 times higher, and their isolation is incredibly simple and efficient (2).

Through their paracrine function, which releases growth hormones and cytokines, research has shown that ADSCs can either directly or indirectly contribute to and assist the regeneration process (17). Additionally, when paired with growth factors, ADSCs can enhance wound healing by promoting angiogenesis and collagen deposition (18).

Platelet-rich plasma (PRP) is a concentrate of platelet-rich plasma protein made from whole blood that has been centrifuged to remove red blood cells (19).

Growth factors and other cytokines present in platelet-derived plasma and autologous conditioned plasma include platelet-derived growth factor (PDGF), fibroblast growth factor (FGF), insulin-like growth factor 1 (IGF-1), insulin-like growth factor 2 (IGF-2), vascular endothelial growth factor (VEGF), epidermal growth factor (EGF), interleukin 8 (IL-8), keratinocyte growth factor (KGF), and connective tissue growth factor (CTGF) (20).

As a result, PRP has been utilized to encourage a rapid healing response in a number of fields, including orthopaedics, dermatology, plastic surgery, and dentistry (2).

It is worthwhile to examine the effects of both on wound healing given the increasing interest in ADSCs and PRP as novel agents in the context of contemporary research for wound healing due to their promising laboratory properties and established results in several specializations.

About 40 male albino rats were used in this experiment; 10 of them served as donors for PRP and ADSCs, while the remaining 30 were split up into three study groups.

The studied groups were:

- Group-I: that included 12 rats treated with ADSCs.
- Group-II: that included 12 rats treated with PRP.
- Group-III: that included 6 control rats.

With the exception of four deaths during wound follow-up (one in group I, one in group II, and two in group III), the rats' survival in every group under study was uneventful.

Every group's wound healing differed significantly over time. At every stage, we discovered that Group I (ADSCs) had the greatest percentage of healing, whereas Group III (control group) had the lowest. Between the control and group I, group II (PRP) was in the middle. All groups saw a rise in the percentage of healing over time, but the rate of increase was greater for groups I and II than for the control group, and it was highest for group I (ADSCs-treated group) throughout.

The healing of a full thickness square wound with a side length of 1 cm was compared between PRP and ADSCs in Zhang et al.'s (2) study. At day three of treatment, there was no discernible difference in wound healing between the control, PRP, and ADSCs groups. Otherwise, starting on day five, the rate of wound healing was higher in the PRP and ADSC-treated groups than in the control group, and it was higher in the ADSC-treated group than in the PRP group.

The comparison between Zhang's study and ours yields three key conclusions. The first is that, with the exception of the rate of healing at day three, when there is a notable variation in the rate of wound healing among all groups, the results of the two trials are rather similar. Second, despite the difference in the intended wound size, the outcomes for the PRP and ADSCs groups in both experiments are extremely similar. Third, our study's control group's rate of wound healing was clearly slower than Zhang et al.'s (2) study. Environmental factors and methodological variations are responsible for all of this.

The incidence of these comments may have been influenced in some manner by the difference in wound size; Zhang et al. (2) utilized a side length of 1 cm for their planned square wound, whereas our investigation employed a side length of 1.5 cm. For example, changes in wound healing may be more noticeable on a bigger scale. The effect of the greater wound defect in our investigation was evident in the control group, where the wider gap significantly impeded the healing process in the absence of any treatment, leading to a more pro-inflammatory wound environment, as indicated by the histology results.

The variations in ADSC and PRP preparation techniques between the two studies can be used to illustrate the following two factors: Zhang et al. (2) cultured ADSCs first, whereas we employed isolated ADSCs immediately in our study. This may prompt us to conduct research comparing the impact of cultured ADSCs against the immediate use of isolated ADSCs on wound healing. In the Zhang et al. (2) study, 0.4 ml (containing 0.4 million cells) were injected uniformly in the wound edges, whereas in our study, 0.5 ml (containing 0.5 million cells) were used, with an additional 0.1 ml being injected into the wound floor. This difference in the amount of ADSCs injected per wound in group I may also be significant. Therefore, compared to Zhang et al.'s (2) work, which used less cultured ADSCs, our investigation used a greater number of freshly separated ADSCs.

In the Zhang et al. (2) study, PRP was prepared using a single centrifugation cycle, whereas in our investigation, it was prepared using two centrifugation cycles. Additionally, our study's PRP injection volume was 0.5 ml, whereas the other study's was 0.4 ml, with an additional 0.1 ml being injected into the wound floor.

Another reason why our study differs from Zhang et al.'s (2) study could be that we injected the wound floor itself with the produced ADSCs or PRP.

Despite the significant variance in wound size, it's possible that all these factors contributed to a high rate of healing in groups I and II from the beginning and throughout our investigation, with results comparable to Zhang et al.'s (2) study.

The fact that Zhang et al. (2) employed adult specific-pathogen-free (SPF) class C57BL/6 mice, whereas our work used adult western albino rats, may also be a contributing factor. The environmental distinctions between Egypt and China, the study's location, may also be relevant.

In a review of histology from animal research on fat grafting, ADSC, and PRP in wound healing, Nolan 2021 noted another important feature. Narrative synthesis was carried out and a literature assessment of significant electronic databases was conducted. Thirty animal studies' worth of data were included. PRP and ADSCs were found to have a greater effect in animals with impaired wound healing, which is a significantly relevant point for the explanation of their robust performance despite the more challenging conditions in the form of increased wound size, synchronous with a significantly hindered rate of healing in the control group (21).

The impact of ADSC on angiogenesis at 7 days in healthy animal subjects varied substantially; two earlier research found no difference in vessel density when compared to negative controls, while three investigations found a considerable rise in vessel density. The fact that healthy animals already recover effectively and have little opportunity for improvement is one explanation for why ADSC proportionately increases angiogenesis more in poor wound healing (21).

According to a study, ADSC-treated diabetic mice outperformed nondiabetic mice in artery density within 7–14 days. The proportional change is low or even zero since healthy animals are already reaching extremely high levels of angiogenesis without ADSC (21).

PRP's impact on the histology of cutaneous tissue also showed enhanced angiogenesis, along with a notable rise in vascular density and granulation tissue thickness (21).

In order to examine the effects of ADSCs and PRP on wound healing, Ni et al. (22) created a diabetic wound model on the backs of SD rats. To cause diabetes, rats were given a single injection of streptozotocin. Rats with hyperglycemia within a week of injection were identified as having diabetes. The circular wounds have a diameter of one centimeter. To avoid contracture, silicone rings were sutured around the wounds. ImageJ software was used to quantify the wound size using digital photos taken on 0, 1, 3, 7, 10, and 14 postoperative days (POD). The outcomes matched those of our investigation. Wound healing was increased by PRP and ADSCs, with the ADSCs group exhibiting the fastest rate of healing. Significant variations between groups were revealed by statistics (22).

In a study carried out in Egypt, Ebrahim et al. (23) examined the effects of PRP and ADSCs on wound healing in an adult albino rat model of diabetes. The rats were given a 0.5 cm circular wound on their backs, and then a sterile donut-shaped silicone splint with a diameter twice that of the wound was fixed with an adhesive film (3MTM Steri-StripTM Skin Closures, 3M Science, Egypt) and interrupted 6-0 silk thread sutures to prevent skin retraction. Evaluation was done both histologically and macroscopically by measuring the rate of wound healing. Similar to our study, both PRP and ADSC treatment of wounds accelerated wound healing when compared to the untreated group; ADSCs produced the best outcomes, and there is a significant difference between all groups at all times.

According to Ebrahim et al.'s (23) macroscopic observation, the diabetes untreated group's wound did not heal by the study's conclusion and continued to exhibit cardinal signs of inflammation. The mean wound healing percentage in the PRP-treated group at the 14th POD was approximately 85%, which is extremely similar to the mean of the PRP group in our study, which is 86.42 +/-1.37. The ADSCs group demonstrated consistent filling of the wound surface with healthy granulation tissue that is quickly covered by epithelium to reduce the wound surface area. This resulted in a wound healing rate of 90% at the 14th POD, which is also close to our study's ADSCs group mean of 94.08 ± 1.37.

Forty Wistar rats were used by Imam and Amer (24), who divided them into four equal groups: control, burn, burn + PRP, and burn + Microvesicles (MVs).Adipose-derived stem cells (ADSC) produce MVs, which are

tiny membrane vesicles with a diameter of 100–1000 nm, to perform their autocrine and paracrine roles. Supernatants of ADSCs cultivated overnight in RPMI without fetal calf serum were used to create MVs. These supernatants were then subjected to a number of centrifugation cycles, washing, microscopic examination, and finally suspending MVs in PBS for wound injection. Rats were sacrificed after small burns were created, their morphology was monitored for three weeks, and the skin lesions were examined using immunohistochemistry and biochemistry. The findings demonstrated that both PRP and MVs influenced the burn healing process, with the MVs group outperforming the PRP group. When compared to the burn and burn + PRP groups, microvesicles dramatically reduced the size of burn wounds at two and three weeks (24).

An experimental investigation comparing the angiogenic effects of PRP and ADSCs in rats was conducted by Morita et al. (25). Seven-week-old male BALB/c nu/nu mice were used to create ischemic hind limb models. These mice were then split into four groups: the control group (n = 3), the rat PRP injection group (n = 3), the rat ADSC-transplanted group (n = 3), and the ADSC-transplanted with PRP injection group (n = 5). Laser doppler blood flow (LBDF) and immunohistochemistry were used to assess the angiogenic effect in each group. On day 28 following ischemia, LDBF revealed that the perfusion recovery in the ADSC-transplanted group was substantially greater than that in the control group, PRP group, and ADSC-transplanted plus PRP injection group. This implies that PRP combined with ADSC transplantation may reduce angiogenesis and endothelial nitric oxide synthase phosphorylation and should be avoided in ischemic limbs (25).

Photomicrographs of sections from each group's excised incision with a skin rim of roughly 1 cm surrounding the wound were used to get the study's histological results on day 14. Additionally, normal skin sections were included in our histological analysis to improve results comparison. First, group I's hematoxylin and eosin study revealed results that were almost identical to those of normal skin in terms of skin adnexa and the thickness of the dermis and epidermis, with the exception of a few areas with slightly thicker dermal fibers; group II also displayed numerous adnexa and fully grown hair, but a thinner epidermis than group I; Additionally, there were less inflammatory cells visible and thicker dermal fibers were visible in several locations compared to group I. Group III had a discontinuous dermo-epidermal connection, the thinnest epidermis, and the largest dermal and glandular infiltration by inflammatory cells.

According to Masson research, groups I and II had more collagen deposition than group III (the control group). The groups' amounts of collagen varied significantly. While groups II and III had far lower levels, group I's results were almost identical to those of unwounded skin.

The levels of +ve PCNA varied significantly amongst the groups. While groups II and III had far greater levels than group I, group I's results were almost identical to those of unwounded skin. Compared to groups I and II, group III's levels were noticeably greater.

The histological results of Zhang et al.'s (2) investigation, which is comparable to ours, revealed that the ADSCs and PRP groups had considerably greater levels of collagen deposition and re-epithelialization than the control group, with the ADSCs group exhibiting the greatest levels.

Hematoxylin and Eosin staining on the 14th POD in Ni et al. (22) revealed that the ADSC's dermis had more appendages and a thicker epidermis than the other groups. Collagen deposition was greater in the PRP and ADSC groups than in the control group and in the ADSCs group than in the PRP group, according to Masson's trichrome staining.

In the Ebrahim et al. (23) investigation, H&E results of skin slices of the untreated group on the 14th POD revealed significant histological changes in the diabetic untreated group, including thin skin that revealed a persistent disruption of the epidermis and delayed wound healing. Pyknotic nuclei were present in the wound bed, and the epidermis on either side of the wound looked disordered with pyknotic nuclei and a continuous lack of keratin. The reticular layer displayed large collagen bundles and less dense collagen fibers, whereas the papillary layer displayed regions of inadequate collagen deposition and a lack of blood capillaries. Persistent inflammatory infiltration was seen in both levels. However, when compared to the diabetes untreated group at the 14th POD, wounds treated with PRP and ADSCs both improved wound healing. The PRP group had a thicker epidermis with

noticeable keratin and keratohyalin granules. Thick bundles of dermal collagen were positioned parallel to the surface. The epidermis seemed thicker and had more noticeable keratin and keratohyalin granules in the ADSCs group. The reticular layer had large bundles of collagen, whereas the papillary layer had more blood vessels and collagen fibers. These findings are comparable to those of our investigation.

According to Imam and Amer's (24) histological findings, the PRP group's H&E staining revealed significant collagen deposition and epithelization. Animals treated with MVs showed complete epithelial layer development, reduced inflammatory cell counts, and clearly visible remodeling of collagen fibrous tissues. The skin of the burned animals showed a significant decrease in fibrous connective tissues, while the skin of the control animals showed normal collagen bundles within the dermal layer using Masson's Trichrome staining. While the skin of burned animals treated with MVs showed significant remodeling and maturation of collagen fibrous tissues, the skin of animals treated with PRP showed significant proliferation of these tissues (24).

The vascular density was higher in the ADSC transplanted group than in the control, PRP, and ADSC transplanted with PRP injection groups, according to a study by Morita et al. (25) that measured capillary density using immunostaining of tissue sections prepared from the thigh adductor muscle of Balb c-nu/nu mice on day 28 with anti-CD31 antibody. This implies that the combination of PRP and ADSC transplantation may reduce angiogenesis and endothelial nitric oxide synthase phosphorylation, and it is preferable to avoid it in ischemic limbs (26).

Conclusion

Our findings suggest the major enhancing functions of ADSCs and PRP in wound healing in rats. More importantly, our study provides compelling clinical and histological evidence that ADSC treatment significantly improves wound healing compared to PRP treatment in a rat model of full-thickness skin wounds. Another noteworthy conclusion is that instantly isolated ADSCs without culture represent a viable strategy for wound healing, with potential benefits in terms of rapid administration, preservation of cellular characteristics, and simpler technique. These findings have significant implications for the development of new treatment techniques to promote wound healing and tissue regeneration in clinical settings. However, more study is needed to improve the separation procedures, describe the cellular characteristics, and assess the long-term efficacy and safety of this therapy approach in preclinical and clinical contexts.

References:

1. Lavrador, P., Marco, R., Vítor, M., et al. (2021). Stimuli-Responsive Nanocomposite Hydrogels for Biomedical Applications. Advanced functional materials; 31(8).
2. Zhang, L., Zhang, B., Liao, B., Yuan, S., Liu, Y., Liao, Z., Cheng, B. (2019). Platelet-rich plasma in combination with adipose-derived stem cells promotes skin wound healing through activating Rho GTPase-mediated signaling pathway. Am J Transl Res.; 11(7):4100-4112.
3. Shennea, S., Ferreyros, M., Kogut, I., et al. (2021). Differentiating Induced Pluripotent Stem Cells Toward Mesenchymal Stem/Stromal Cells. Methods in molecular biology; 11(20): 9755.
4. Ong, W.K. and Sugii, S. (2013). Adipose-derived stem cells: fatty potentials for therapy. Int J Biochem Cell Biol; 45: 1083-1086.
5. Kloskowski, T., Kowalczyk, T., Nowacki, M. and Drewa, T. (2013). Tissue engineering and ureter regeneration: is it possible? Int J Artif Organs; 36: 392-405.
6. Chu, C., Wei, S., Wang, Y., et al. (2018). Extracellular vesicle and mesenchymal stem cells in bone regeneration: recent progress and perspectives. Journal of Biomedical materials research; 107(1); 243-250.
7. Hong, S.J., Jia, S.X., Xie, P., Xu, W., Leung, K.P., Mustoe, T.A., et al. (2013). Topically delivered adipose derived stem cells show an activated-fibroblast phenotype and enhance granulation tissue formation in skin wounds. PLoS One; 8: e55640.
8. Cecerska, E., Goszka, M., Serwin, N., et al. (2021). Applications of the regenerative capacity of platelets in modern medicine. Cytokine & Growth Factor Reviews; 61: 27-37.

9. Lu, F., Mizuno, H., Uysal, C., Cai, X., Ogawa, R., Hyakusoku, H., et al. (2008). Improved Viability of Random Pattern Skin Flaps through the Use of Adipose-Derived Stem Cells. Plast. Reconstr. Surg. 121: 50-58.
10. Schimandle, J. H., & Boden, S. D. (1994). Spine update animal use in spinal research. Spine, 19(21), 2474-2477.
11. Gomes, P. S., & Fernandes, M. H. (2011). Rodent models in bone-related research: the relevance of calvarial defects in the assessment of bone regeneration strategies. Laboratory animals, 45(1), 14-24.
12. Nguyen, A.V., Soulika, A.M. (2019). The Dynamics of the Skin's Immune System. International Journal of Molecular Sciences; 20(8):1811.
13. Kolimi, P., Narala, S., Nyavanandi, D., Youssef, A.A.A., Dudhipala, N. (2022). Innovative Treatment Strategies to Accelerate Wound Healing: Trajectory and Recent Advancements. Cells; 11(15):2439.
14. Vasalou, V., Kotidis, E., Tatsis, D., Boulogeorgou, K., Grivas, I., Koliakos, G., ... & Angelopoulos, S. (2023). The effects of tissue healing factors in wound repair involving absorbable meshes: a narrative review. Journal of clinical medicine, 12(17), 5683.
15. Kangari, P., Talaei-Khozani, T., Razeghian-Jahromi, I. et al. (2020). Mesenchymal stem cells: amazing remedies for bone and cartilage defects. Stem Cell Res Ther 11, 492.
16. Gou, Y., Yanran, H., Wenping, L., Yanan, L., Piao, Z., Jiamin, Z., Xiangyu, D., Meichun, G., Aohua, L., Ailing, H., Guozhi, Z., Yonghui, W., Yi, Z., Hui, Z., Yunhan, S., William, W., Hue, H.L., Lewis, L.S., Russell, R.R., Tong-Chuan, H., Jiaming, F. (2023). Adipose-derived mesenchymal stem cells (MSCs) are a superior cell source for bone tissue engineering, Bioactive Materials, 34: 51-63.
17. Qin Y, Ge, G., Yang, P., Wang, L., Qiao, Y., Pan, G., Yang, H., Bai, J., Cui, W., Geng, D. (2023). An Update on Adipose-Derived Stem Cells for Regenerative Medicine: Where Challenge Meets Opportunity. Adv. Sci., 10, 2207334.
18. Hao, Z., Qi, W., Sun, J., Zhou, M., Guo, N. (2023). Review: Research progress of adipose-derived stem cells in the treatment of chronic wounds. Front Chem.; 11:1094693.
19. Collins, T., Alexander, D., & Barkatali, B. (2021). Platelet-rich plasma: a narrative review. EFORT Open Reviews, 6(4), 225-235.
20. Verma, R., Kumar, S., Garg, P. et al. (2023). Platelet-rich plasma: a comparative and economical therapy for wound healing and tissue regeneration. Cell Tissue Bank 24, 285–306.
21. Nolan, G. S., Smith, O. J., Jell, G., & Mosahebi, A. (2021). Fat grafting and platelet-rich plasma in wound healing: a review of histology from animal studies. Adipocyte, 10(1), 80–90.
22. Ni, X., Shan, X., Xu, L. et al. (2021). Adipose-derived stem cells combined with platelet-rich plasma enhance wound healing in a rat model of full-thickness skin defects. Stem Cell Res Ther; 12, 226.
23. Ebrahim, N., Dessouky, A.A., Mostafa, O. et al. (2021). Adipose mesenchymal stem cells combined with platelet-rich plasma accelerate diabetic wound healing by modulating the Notch pathway. Stem Cell Res Ther 12, 392.
24. Imam, R.A., Amer, M.M. (2023). Potential therapeutic role of microvesicles derived from mesenchymal stem cells and platelet-rich plasma in murine burn wound healing: scar regulation and antioxidant mechanism. Folia Morphol (Warsz).; 82(3):656-667.
25. Morita, M., Damle, E. B., Shinohara, I., Murayama, M., Susuki, Y., Gao, Q., ... & Goodman, S. B. (2023). Targeting cellular senescence in progenitor cells as a strategy to enhance bone regeneration by cell therapies: a systematic review of pre-clinical investigations. Stem Cell Research & Therapy, 16(1), 669.
26. Josh, F., Soekamto, T.H., Adriani, J.R., et al. (2021). The combination of stromal vascular fraction cells and platelet-rich plasma reduces malondialdehyde and nitric oxide levels in deep dermal burn injury. J Inflamm Res.; 14:3049–3061.